Properly designed temperature history nanoparticles may improve residual oil saturation estimates from SWCT tests

Tom Pedersen

Department of tracer technology
Institute for energy technology
P.O. Box 40
2027 Kjeller
Norway
+47 47 94 97 95

tom082012@gmail.com

www.ife.no

Corresponding author: Tom Pedersen
tom082012@gmail.com

Abstract

Considerable resources are required to develop new nanoparticles for various applications. Before too much effort is put into the development of nanoparticles that might not work properly, it may be wise to spend more resources on studies of how they should de designed to be really useful for solving an identified problem. In particular, we believe that it is a good idea to demonstrate the usefulness of as yet hypothetical nanoparticles by performing computer simulations of the system at hand with them. To exemplify this idea, we use the so-called Single Well Chemical Tracer (SWCT) test, the purpose of which is to estimate the residual oil saturation (S_{or}) in the vicinity of a wellbore. In the majority of reported SWCT tests, ethyl acetate is pushed into the oil bearing formation from a well and partly converted to ethanol by hydrolysis. The chromatographic separation between the ethyl acetate and ethanol during back production is then used to estimate S_{or}. The hydrolysis rate of ethyl acetate depends exponentially on temperature, and if a temperature gradient develops across the ethyl acetate bank, this has to be accounted for if a correct S_{or} estimate shall be obtained. Nanoparticles that are co-injected with the ethyl acetate and that have a 'memory' of the temperature history they have experienced may prove useful in this respect. We suggest several design criteria for such nanoparticles. The envisioned nanoparticles encapsulate a dye that degrades when heated as well as an internal standard that does not degrade. This property facilitates easy calibration of the fluorescence signal. We propose a simple rule for deriving degradation rates suitable for the temperatures and times typical for a SWCT test. The nanoparticles move with the ethyl acetate so that their temperature history is representative for its hydrolysis. It is important that it is easy and uncostly to analyze the temperature history nanoparticles. They have to satisfy modern health, safety and the environment (HSE) requirements, and have acceptable production and deployment costs. An axis-symmetrical numerical model is used to demonstrate the usefulness of such designed nanoparticles based on data from a published SWCT test. First, we calculate the temperature history of the nanoparticles using a suite of injection temperatures. The pre-exponential factor and activation energy of the dye derived from the design criteria are then used to simulate the degradation in nanoparticle fluorescence with time for the various nanoparticle temperature histories. From these data, we calculate the aggregate average and standard deviation of the nanoparticles' fluorescence in the produced fluid, i.e., information that would be available if the nanoparticles had been used in a real SWCT test. We find that such data provide useful constraints on the temperature history and thus helps us pin-point the correct S_{or} value. The temperature history sensitive nanoparticles may potentially also yield valuable information on the effective thickness and other characteristics of the target formation, the surrounding rock and perhaps even on the wellbore and its thermal interaction with the reservoir rocks.

Keywords

Residual oil saturation; Single well chemical tracer test; Temperature history; Intelligent nanoparticles; Fluorescence.

1. Introduction

The various types of nanoparticles aimed at solving problems in almost all kinds of enterprises are innumerable. The oil industry is no exception, and nanoparticles are being developed that

hopefully will be useful in petroleum exploration, drilling, exploitation and distribution (e.g., Kong and Mohadi, 2010) just to mention some potential application areas. However, it seems fair to say that real progress has not been as rapid as many had hoped (Friedheim et al., 2012). Reports do exist on nanoparticle design, synthesis and characterization for specific oil and gas applications (e.g., Fletcher and Davis, 2010). However, much of this work is empirical in nature. The time and money needed to develop new particles are substantial and in our view it may be wise to reallocate more resources into studies of how particles should de designed in order to be really useful for solving an identified problem. In this way, research on new nanoparticles can be guided in the right direction, potentially saving time as well as money. Especially, it may be a good idea to perform computer simulations of the system at hand with as yet hypothetical nanoparticles in order to examine their usefulness.

In this paper, we discuss an important, well-defined and relatively simple system - the so-called Single Well Chemical Tracer (SWCT) test, the purpose of which is to estimate the residual oil saturation (S_{or}) in a reservoir (Deans, 1971). The S_{or} concept is used in several ways in the literature, including 'irreducible oil saturation', and 'oil saturation in swept zones after a water flood' (Interstate Oil Compact Commission, 1978). How close these meanings are depends on wettability and other factors like the viscosity of the oil. In water-wet rocks with a low viscosity oil, irreducible oil saturation by water injection may be reached after just one pore volume of water has been pumped through, whereas in mixed-wettability rocks, thousands of pore volumes of water may be required before there is no more mobile oil left (Salathiel, 1973). It is S_{or} in the first sense that corresponds to zero relative oil permeability (cf., Wyckoff and Botset, 1936). In practice, a low oil-cut of about 2% is considered acceptable (e.g., Deans and Majoros, 1980).

Reliable S_{or} estimates are important for calculating recoverable reserves, planning water floods and in Enhanced Oil Recovery (EOR) operations. How much residual oil there is, and where it is, will often govern the most efficient way of conducting the operations. Core analysis and well logging are the most straightforward and common methods used to estimate S_{or}. It is, however, challenging to take and maintain cores at reservoir conditions. Logging may be expensive and the results obscured by formation damage near the wellbore. Moreover, these methods provide a S_{or} estimate based on only a small rock volume close to the wellbore, and it is difficult to know how representative the result is for the surrounding reservoir. The SWCT method, pioneered in the late 60's by the Exxon Production Research Co. (Deans, 1971), yields on the other hand an average S_{or} based on a large volume of rock, typically several hundred cubic meters, with a horizontal depth of penetration of ~3-12 meters away from the well, and a vertical dimension of several meters. This large sampling volume, together with the ability to control the depth of investigation, may be considered the main advantages of the SWCT method relative to other techniques (Sheely and Baldwin, 1982).

A SWCT test consists of four steps – injection, push, shut-in (or soak) and production. Typically, the test starts with injection of a partitioning (water-and-oil-soluble) tracer like ethyl acetate (primary tracer) dissolved in brine into the oil-bearing formation. The primary tracer bank is then pushed further into the target formation by subsequent injection of tracer-free brine. Thereafter, there is a few (~2-12) days shut-in during which the primary tracer is partially converted into a secondary tracer by hydrolysis - ethanol in the case of ethyl acetate. The secondary tracer is non-partitioning (water-soluble-only), also referred to as an ideal water tracer

since it moves with the water. Another version of the SWCT method is to inject halogen-acid salts that generate CO_2 (Wellington and Richardson, 1994). Here, the primary tracer moves with the water and the secondary tracer partitions to the oil. In this contribution, we focus on the ethyl acetate-ethanol method.
When back-production commences, both ethanol and ethyl acetate move towards the wellbore. Since ethanol moves with the water, and the ethyl acetate spends some of its time in the immobile oil, ethyl acetate is delayed relative to ethanol. How much depends on S_{or}. The concentrations of the two tracers are monitored at the well and plotted as a function of produced volume. Interpretation of the tracer curves may be performed by simple analytical expressions or advanced computer simulations (e.g., Deans and Majoros, 1980). In favourable cases, a SWCT test accuracy of about 2 to 3% is confirmed by laboratory results from pressure-core methods (Tomich et al., 1973). The SWCT method has become popular, and we estimate that close to one thousand SWCT tests have been performed worldwide.

The injected brine that contains the tracers is normally colder than the temperature in the oil bearing formation. Tezduyar et al. (1987), Park (1989), Park et al. (1990) and Park et al. (1991) developed non-isothermal convection-diffusion-reaction finite-element numerical models of SWCT tests solving for the concentrations of primary and secondary tracers as well as temperature. They found that the temperature front is retarded relative to the water front. How much depends on the thermal properties of the rocks and brine, formation thicknesses, injection rates, duration of the various periods, etc. (Park, 1989; Tezduyar et al., 1991). In many cases, the velocity of the temperature front is such that a temperature gradient develops across the primary tracer bank (Fig. 1).

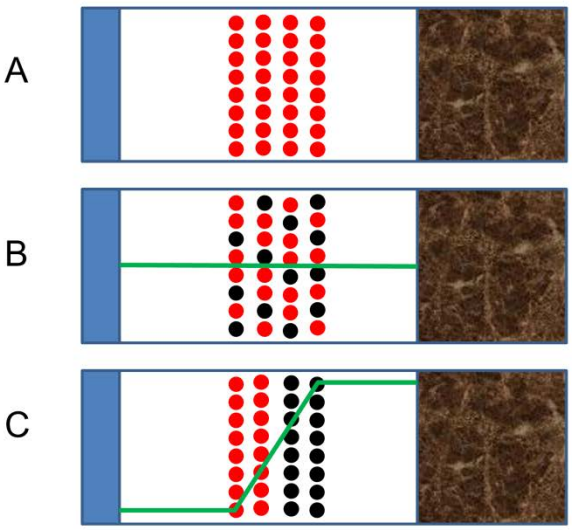

Figure 1. Schematic illustration of the temperature gradient that may develop across the primary tracer bank in a SWCT test. The white area represents the injected brine. The primary tracer (red dots) is injected into the permeable formation believed to contain residual oil (A). The primary tracer is partly converted into a secondary tracer (black dots). If the temperature (green line) across the primary tracer bank is constant, the primary and secondary tracers are located at the same distance from the wellbore (B). However, if there is a temperature gradient across the primary tracer bank, the location of the secondary tracer will be displaced further away from the wellbore (C).

Since the primary tracer hydrolysis rate increases exponentially with temperature (Deans and Majoros, 1980), such a gradient will cause the concentration peak of the secondary tracer to be located significantly further away from the well than the peak of the primary tracer. When the tracer concentrations subsequently are measured at the well site, this 'handicap' will reduce the observed time difference between the primary and secondary tracers and this may translate into erroneous S_{or} estimates if the effect isn't accounted for.

Alas, these authors did not have the necessary independent information to mathematically constrain the temperature histories during a SWCT test (i.e., implausible histories are identified and eliminated because they are not consistent with the available information). This may be one reason why non-isothermal temperature effects are mostly ignored in SWCT tests. If a methodology can be devised that allows us to put constraints on the temperature history, this may have several important implications. For example, if the 'observed' temperature history is different from the modelled temperature history, we know that there is something wrong with the model. The estimated temperature with which the injection fluid enters the target formation may be too high or too low, or perhaps the effective thickness of the target formation (i.e., where the flow, or at least most of it, actually takes place) is lower or higher than believed due to geological structures, permeability heterogeneities, diagenetic processes or faults and fractures. A number of other parameters like for example the thermal conductivity of the fluids and rocks also influence the temperature history. Systematically changing model parameters until a good fit between observed and calculated temperature histories as revealed by the nanoparticles is obtained should improve the SWCT model, and thus potentially the S_{or} estimate. The extra cost of such work will probably be insignificant relative to the potential gain and cost of the SWCT test itself. As a by-product, non-isothermal SWCT models may reveal interesting information on the wellbore and its thermal interactions with the surrounding rock. Also in the planning phase of a SWCT test, such models may prove valuable.

In this paper, we discuss how nanoparticles that are co-injected with the primary tracer should be designed so that they can provide information on the temperature history, and thus hydrolysis rate, during a SWCT test.(In that realm, the nanoparticles could equally well been called nanotracers, but we prefer to use the more general term.) Nanoparticles have many attractive features pertaining to this kind of investigations including the possibility to design particles with various sizes, functionalities (i.e., what they measure), encapsulations and surface functionalization. Moreover, several of the required nanoparticle characteristics have already been realized (e.g., Agenet et al., 2012), strengthening our belief in the realism of the proposed nanoparticles. This does not exclude the possibility of developing for example molecules that might be used instead. It is beyond the scope of this contribution to discuss the relative merits of molecules versus nanoparticles in SWCT tests. Notwithstanding, we note that encapsulating for instance a dye within a nanoparticle might offer better protection against hot and aggressive reservoir fluids than a molecule may provide.

We demonstrate the usefulness of the as yet hypothetical nanoparticles with data from a real SWCT test. Availability of 'temperature history' nanoparticles may perhaps encourage service companies and others to include temperature effects in their SWCT test planning and result interpretation.

2. Design of temperature history nanoparticles for SWCT tests

Nanoparticles that can be used as constraints on the temperature history of fluids, more specifically the primary tracer's temperature history, used in a SWCT test should or must fulfill several criteria:

1. They must have a component that responds irreversibly to heating. Otherwise, the particle will have no memory of the temperature in the target formation during the SWCT test. We think that a fluorescent dye might be ideal for this purpose. Dyes, and in particular fluorescein, are used as tracers in groundwater and geothermal systems because of their low detection limits, ease of analysis, resistance to biodegradation and insensitivity to variations in water chemistry (Adams and Davis, 1991). However, fluorescein and other fluorescent dyes are known to adsorb on sediments (Smart and Laidlaw, 1977) and their often low recovery (i.e., the percentage of injected fluorescein that is back-produced) may make their quantitative interpretation difficult. Encapsulating the dye within a nanoparticle could reduce or eliminate these problems. Hereafter, we discuss only fluorescent nanoparticles because of their many attractive features. Obviously, other possibilities exist.

2. The nanoparticles should also have an internal standard or reference fluorescent component that does not degrade upon heating (e.g., Agenet et al., 2012). The reference facilitates the quantification of the decrease in fluorescence in a sample with many nanoparticles that is caused by heating.

3. They should be easy to analyze. Fluorescent nanoparticles can be analyzed in a quite simple, rapid and cost-effective way when they return from the reservoir. One problem might be background noise caused by hydrocarbons in the produced fluid. However, since we assume a very low oil cut, this problem should not be too serious. To the extent that this is a problem, it will probably be possible to solve by separation methods.

4. The degradation rate of the temperature sensitive fluorescent component must be sufficiently rapid for measurable changes to be observed for the times and temperatures pertaining to SWCT tests. On the other hand, it must not be so rapid that there is no more fluorescence left to measure. A simple and practical way of obtaining this might be to observe the following two criteria (there are, of course, numerous other possibilities): A. There is a 10% reduction in fluorescence after the duration of SWCT test when the lowest realistic temperature is used in the calculations of the thermal decay of the nanoparticles. B. There is a 90% reduction when the highest realistic temperature is used. This should assure that we will get interpretable results. The lowest realistic temperature may be the fluid temperature at the top of the wellbore and the maximum temperature the ambient temperature in the reservoir. Provided that the degradation of

the dye or another temperature sensitive component follows Arrhenius kinetics, these two constraints will be sufficient to uniquely determine the pre-exponential factor and the activation energy.

5. Fluorescence degradation should depend on time and temperature only and not for instance on oxygen content since this might severely complicate the interpretation of the fluorescence data. For example, according to Adams and Davies (1991) the half-life of fluorescein in distilled water is increased from about eight hours with an oxygen content around 6.9 ppm to 130 years for an oxygen content less than 0.1 ppm, i.e., a factor of 140 thousand. SWCT tests are executed with a range of different brines and their oxygen content varies widely (Sven Hartvig, pers. comm., 2017). In addition, it may be difficult to estimate how the oxygen content varies in the wellbore as well as in the formation. For this reason, it is highly desirable, perhaps even a requirement that the fluorescence degradation rate of the dye (or any other temperature sensitive component for that matter) depends on temperature only.

6. The nanoparticles must be able to travel with the injection fluids through the porous rock. One obvious requirement is that the nanoparticles have a sufficiently small diameter so that they can pass through the pore throats in the oil bearing formation without plugging them. However, the nanoparticles should be significantly smaller than the pore throats, perhaps one-fifth or one-seventh to avoid bridging (a well-known phenomenon in sand control) (e.g., Kanji et al., 2009). In siliciclastic reservoirs, a diameter of about 100-1000 nm or less should then be sufficient for medium or fine sandstones whereas in tight sandstones a diameter of only 1-100 nm may be required (cf. Nelson, 2009). In the ARAB-D formation in the dolomite-limestone Ghawar field in Saudi Arabia, Kanji et al. (2009) argue from pore-throat considerations that nanoparticles should be smaller than about 70-100 nm in diameter.

Two other factors that affect nanoparticle transport in reservoirs are particle aggregation and deposition on rock or oil coated surfaces. Quantitative considerations encompass relatively simple Derjaguin, Landau, Vervey and Overbeek (DLVO) calculations and complex numerical models (e.g., Elimelech et al., 1995). Evaluating the various techniques and their application to nanoparticle transport in reservoirs is beyond the scope of this study, but a quite straightforward and practical approach may be to manipulate the nanoparticles' zeta potential and execute flooding experiments until satisfactory results are obtained (Yu et al., 2010).

7. The distribution constant (partition coefficient), i.e., the concentration of the particles in the residual oil divided by their concentration in the brine, must be known, since this determines how fast the particles will move relative to the injection fluid (chromatographic effect). Intuitively, it seems preferable that the particles have a distribution constant close to that of the primary tracer, since it is the temperature history of the primary tracer bank that is most important. If for example, the nanoparticles have a distribution constant close to zero, they will move ahead of the temperature front, and the fluorescence degradation will be dominated by the temperature in the oil bearing formation (cf., Park et al., 1991). We note in passing, that such nanoparticles could be useful in the halogen-acid salts-CO_2 method mentioned above since there the primary tracer follows the water.

8. The nanoparticles will have to fulfill human health, safety and the environment (HSE) criteria. If not, the proper authorities and others will not permit their production, transport or use. It is clearly advantageous to take these considerations into account at an early stage in the development of the particles before too many resources have been spent. The so-called 'Safe by Design' approach (e.g., Fadeel, 2013) is becoming increasingly popular in this respect. The goal of this methodology is to select the most promising nanoparticle candidates already at the design stage. By investigating nanoparticle prototypes and study how their properties change in relevant environments (formation water, rock type, etc.), and how this impacts their HSE characteristics, further development can be guided in fruitful directions.

9. Last, but not least, are of course cost considerations. Nanoparticles may be low-cost compounds. The 'A-Dot' nanoparticles developed by Saudi Aramco can probably be produced at a cost of less than $10 per kilo (Rassenfoss, 2012). Although the temperature history nanoparticles may be more expensive than this, the very low detection limits of the dyes encapsulated in the nanoparticles imply very low concentrations and thus small volumes. Once nanoparticles start to be produced in an industrial manner, their cost is likely to fall rapidly. It will probably be possible to analyze the nanoparticles on-line or in-line so that the time-consuming and costly procedure of sending samples to a laboratory for analysis can be avoided.

3. Demonstration of the usefulness of the designed nanoparticles

We now turn to a demonstration of the usefulness of nanoparticles designed as discussed above in the realm of a SWCT test. A finite-element numerical non-isothermal model of a SWCT test is used to calculate synthetic temperature histories of the nanoparticles as well as their reduction in fluorescence. We use Field Test #3 in Deans and Majoros (1980) to exemplify the applicability of this technology. All the fundamental assumptions of the SWCT method seem to be fulfilled in this 'ideal' test (Deans and Majoros, 1980). Field Test #3 has been much discussed in the literature, and it is thus unnecessary for us to duplicate work already performed. Fig. 2 shows the estimated S_{or} as a function of injection temperature (Park, 1989). This figure clearly shows that the estimate depends on the assumed injection temperature. Importantly, there is no discernible difference between the fit of the various injection temperature models to the observed primary and secondary tracer curves (Park, 1989). Consequently, some kind of independent information is required to select the correct S_{or}. Unfortunately, since Park (1989) did not have such information, she could not determine which was the best S_{or} estimate. This study will demonstrate that nanoparticles that have a memory of their temperature history during a SWCT test may fill this gap.

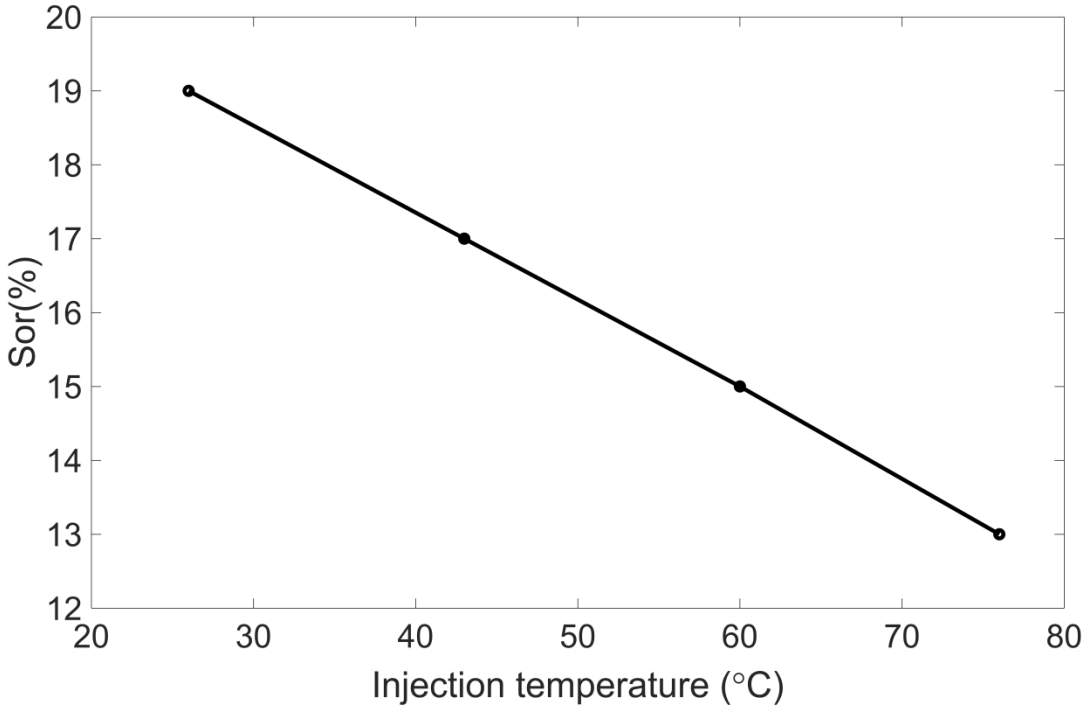

Figure 2. Estimated Sor as function of injection temperature for Field Test #3 in Deans and Majoros (1980). Based on Park (1989). The reservoir temperature is 76 °C.

Our starting point is the model presented in Park (1989). Since radial flow is typical for SWCT tests, it is numerically advantageous to have an axis-symmetrical model centered on the vertical wellbore (Fig. 3).

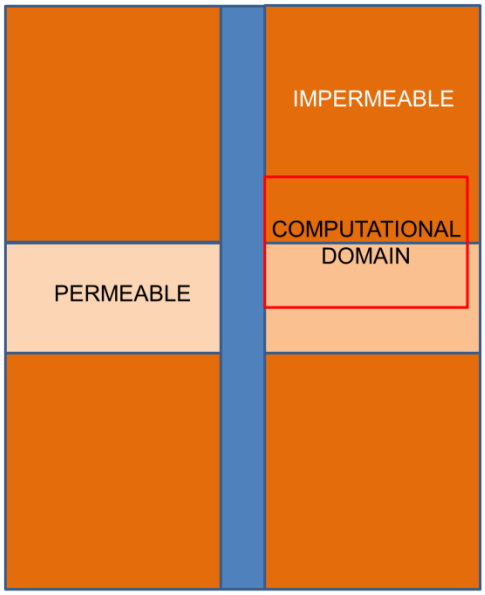

Figure 3. The SWCT model configuration. The permeable target formation is surrounded by impermeable rock. Symmetry makes it possible to solve the equations only for the red box labeled COMPUTATIONAL DOMAIN. The wellbore is in blue.

Such a geometry makes it possible to take three-dimensional effects into account in a simple and efficient manner. Three horizontal rock units surround the well. The formation where we wish to estimate S_{or} is a sandstone unit with a high permeability. Above and below this layer there are impermeable shales with equal thicknesses (model parameters are given in Table 1).

Symbol	Value	Description
A	133 1/s	Pre exponential factor
A_{np}	$3.14\ 10^{-14}$ m^2	Nanoparticle surface area
C_{np}	2200 J/K kg	Nanoparticle heat capacity
D_L	10^{-8}-10^{-10} m^2/s	Longitudinal dispersion coefficient
D_m	$5.1\ 10^{-12}$ m^2/s	Diffusion constant
Ea	53445 J/mol K	Activation energy
H	6.1 m	Target formation height
I		Fluorecence
I_0	1	Initial fluorescence
K_{np}	6.7	Nanoparticle distribution constant
qinj	$1.84\ 10^{-3}$ m^3/s	Injection rate

qprod	1.20 10^{-3} m^3/s	Production rate
R	8.314 J/mol	Universal gas constant
Rc		Retardation factor
Sor	13-19%	Residual oil saturation
T		Temperature
TI	26-76 °C	Injection temperature
tinj	1 day	Injection period
tprod	6 days	Production period
tpush	1 day	Push period
tshutin	12 days	Shut-in period
TR	76 °C	Reservoir temperature
ϕ	0.34	Target formation porosity
η	10^{-3} Pa s	Fluid viscosity
u		Darcy velocity
v		Interstitial velocity
$(\rho C_p)_{oil}$	1.67 10^6 $J/m^3/K$	Oil volumetric heat capacity
$(\rho C_p)_{rock}$	2.41 10^6 $J/m^3/K$	Rock volumetric heat capacity
$(\rho C_p)_{water}$	4.18 10^6 $J/m^3/K$	Water volumetric heat capacity
h	500 W/Km^2	Heat transfer coefficient
k_B	1.38 $m^2kg/s\,K$	Boltzmann' constant
k_{eff}	2.45 W/m K	Effective thermal conductivity
m_{np}	1.1510^{-8} kg	Nanoparticle mass

Table 1. Symbols, values and descriptions.

The symmetry of the model makes it possible to solve the equations within the computational domain illustrated in Figs. 3 and 4, only. The commercial partial differential equations software package COMSOL Multiphysics (2016) is used to build the model, solve the equations and for post-processing.

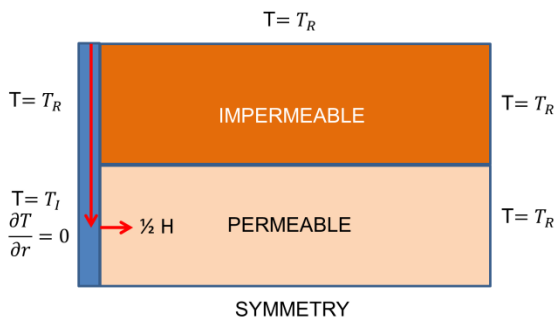

Figure 4. Numerical model used to calculate the temperature history of nanoparticles injected during a SWCT test. The injection fluid (red arrows) flows down the wellbore and into the permeable layer with a temperature TI. When shut-in commences, this boundary condition is changed to a zero temperature gradient (Neumann type condition). The other thermal boundary conditions are of the Dirichlet type. The initial temperature is everywhere equal to the reservoir temperature TR. This is realistic since the vertical extent of the computational domain is small.

We assume, like Park (1989), Park et al. (1990) and Park et al. (1991) that the target formation and the adjacent impermeable layers are at thermal equilibrium (T≡TR) when the calculations commence (Fig. 4). This assumption will not be valid if the SWCT test *sensu stricto* follows pre-injection of a tracer free fluid. If that is the case, the thermal simulations have to start when the pre-flush begins. We note that pre-flushing may strip off light components in the residual oil, and thus change its composition and S_{or} (Gadgil, 1979; Deans and Majoros, 1980).

The injected brine flows into the permeable layer from the left (Fig. 4). For perfect radial flow of an incompressible fluid, the Darcy radial velocity (component), u, as a function of distance, r, from the wellbore is:

$$u = Q/2\pi H(r + r_0) \tag{1}$$

where Q is the pumping rate, r_0 is the wellbore radius and H is the thickness of the permeable layer (Park, 1989).

The temperature during the SWCT test, T, is calculated from the equation

$$(\rho C_p)_{eff}\frac{\partial T}{\partial t} + (\rho C_p)_{water} u\nabla T = \nabla(k_{eff}\nabla T) \tag{2}$$

in which t is time, ρ is density, C_p is heat capacity at constant pressure and u is again the Darcy velocity.

The effective volumetric heat capacity is

$$(\rho C_p)_{eff} = (1-\theta)(\rho C_p)_{rock} + \theta\{(\rho C_p)_{oil} S_{or} + (\rho C_p)_{water}(1-S_{or})\} \quad (3)$$

where θ is the porosity, ρ and C_p the density and heat capacity, respectively (Table 1).

The thermal boundary conditions during the various phases are illustrated in Fig. 4. We do not solve the equations for the concentration of the primary and secondary tracers as this has already been done by Park (1989) for exactly the same model parameters that we use.

The nanoparticles radial velocity v, is equal to:

$$v = u/\theta R_C(1-S_{or}) \quad (4)$$

where again θ is porosity and R_c is the chromatographic retardation factor (e.g., Deans and Majoros, 1980),

$$R_c = 1 + K_{np} S_{or}/(1-S_{or}) \quad (5)$$

in which K_{np} is the nanoparticle's distribution constant between oil and brine.

The nanoparticles interact thermally with the surrounding fluid according to the equation (McAdams, 1954):

$$m_p C_p dT_p/dt = hA_p(T-T_p) \quad (6)$$

Here, T_p is particle temperature, t is time, T is fluid temperature, m_p and C_p are the mass and specific heat of the particle, respectively, h is the heat transfer coefficient and A_p is the particle's surface area. We have selected a particle diameter of 100 nm and h equal to 500 (W/m^2K). A 100 nm nanoparticle should have good transport properties in many siliclastic (Nelson, 2009) and carbonate (Kanji et al., 2009) reservoirs. The exact value of h is immaterial in this case. Due to their small size, the nanoparticles are essentially in thermal equilibrium with the fluid.

Assuming that the fluorescence of the temperature sensitive component in the particle, I, degrades with time as a first-order reaction with a constant rate constant, k, we have that (e.g., Adams and Davis, 1991)

$$I = I_o exp(-kt) \quad (7)$$

where I_0 is the initial fluorescence. For simplicity, we set I_0 equal to one. We further assume that the degradation follows Arrhenius kinetics, i.e,

$$k = Aexp(-E_a/RT) \quad (8)$$

in which A is the pre-exponential factor, E_a is the activation energy, R is the universal gas constant, and T is the temperature in K (e.g., Adams and Davis, 1991).

Before we can calculate the thermal decay of the dye within the nanoparticles, we need values for A and E_a. With two unknowns, two constraints are needed. Using the criteria discussed in #4 above, i.e., 1) there is a 10% reduction in fluorescence after 20 days (the duration of the test (Table 1)) for a constant temperature equal to the injection temperature, and 90% reduction with the highest temperature, we find that A=133 s^{-1} and E_a=53442 J/mol. Fig. 5 shows the degradation half-life of the dye as a function of temperature with these parameters.

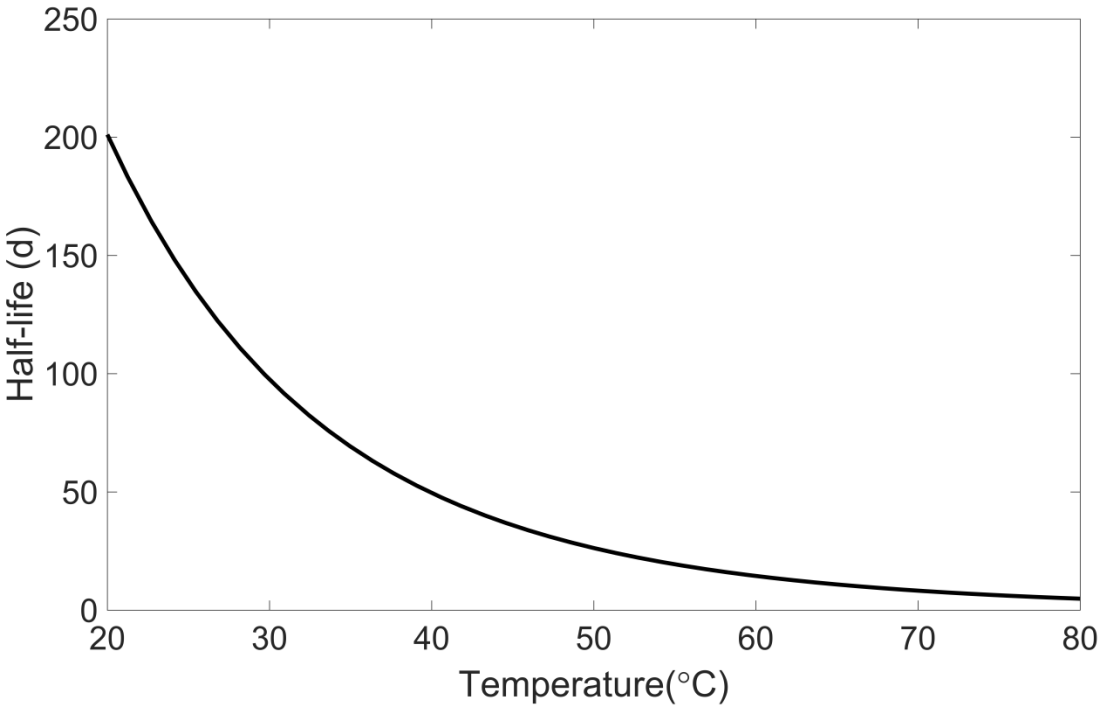

Figure 5. Half-life of dye within a temperature nanotracer using the pre-exponential factor and activation energy derived as discussed in the text.

The 'hypothetical' nanoparticles are co-injected with the primary ethyl acetate tracer. After some experimentation, we found that using 100 nanoparticles evenly distributed in time (one day) and space was sufficient to provide a representative picture of the temperature history of the ethyl acetate tracer bank.

4. Results

Fig. 6 illustrates temperature as function of distance from the well after two days (end of injection and push periods) for various injection temperatures. The temperature gradient across the primary tracer increases with lower injection temperature. Since the hydrolysis rate increases exponentially with temperature, this implies that the lower the injection temperature is, the

further from the well will the bulk of the secondary tracer be located. A fixed observed time difference between the produced primary and secondary tracers will hence correspond to higher and higher S_{or} values. The curves are labeled with the S_{or} estimates of Park (1989) (cf., Fig. 2).

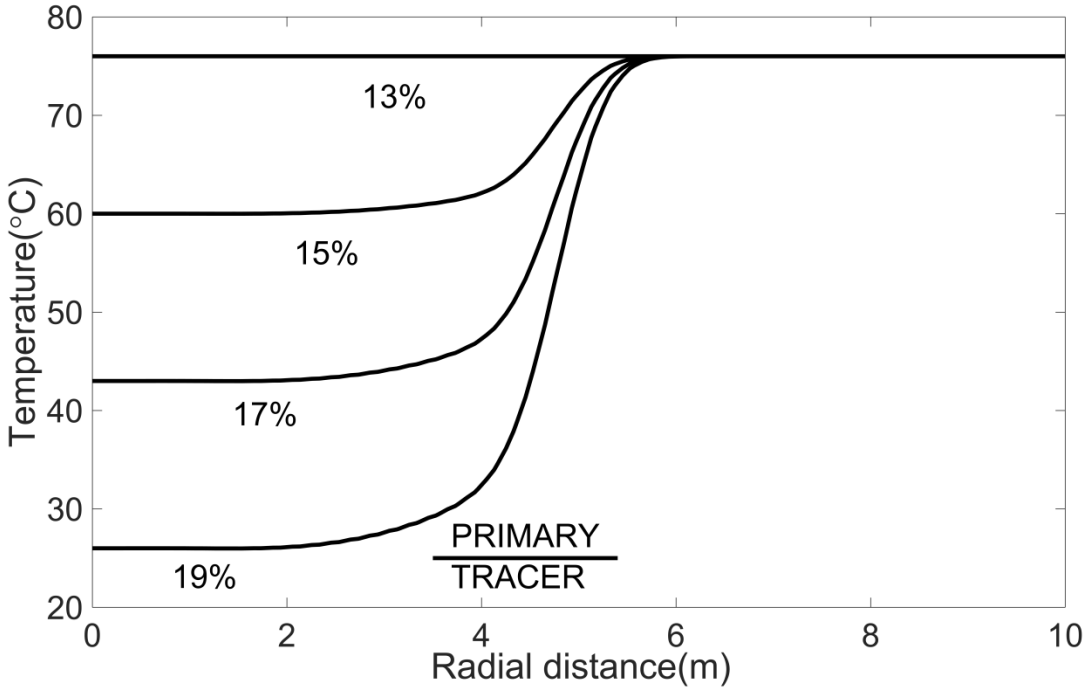

Figure 6. Temperature profiles across primary tracer bank after two days (injection and push). The percentages refer to estimated S_{or} in Field Test#3 in Park (1989). The reservoir temperature is 76 °C.

The temperature of the injected nanoparticles as a function of time (Eq. 6) is depicted in Fig. 7. The temperature history of individual particles depends on their distance to the hot impermeable layers and their distance from the waterfront. In the temperature calculation, we assume that when the particles return to the SWCT test well, they will keep their temperature for the duration of the test. In reality, the particles will cool off rapidly as they move upwards in the wellbore and towards the relatively cold surface.

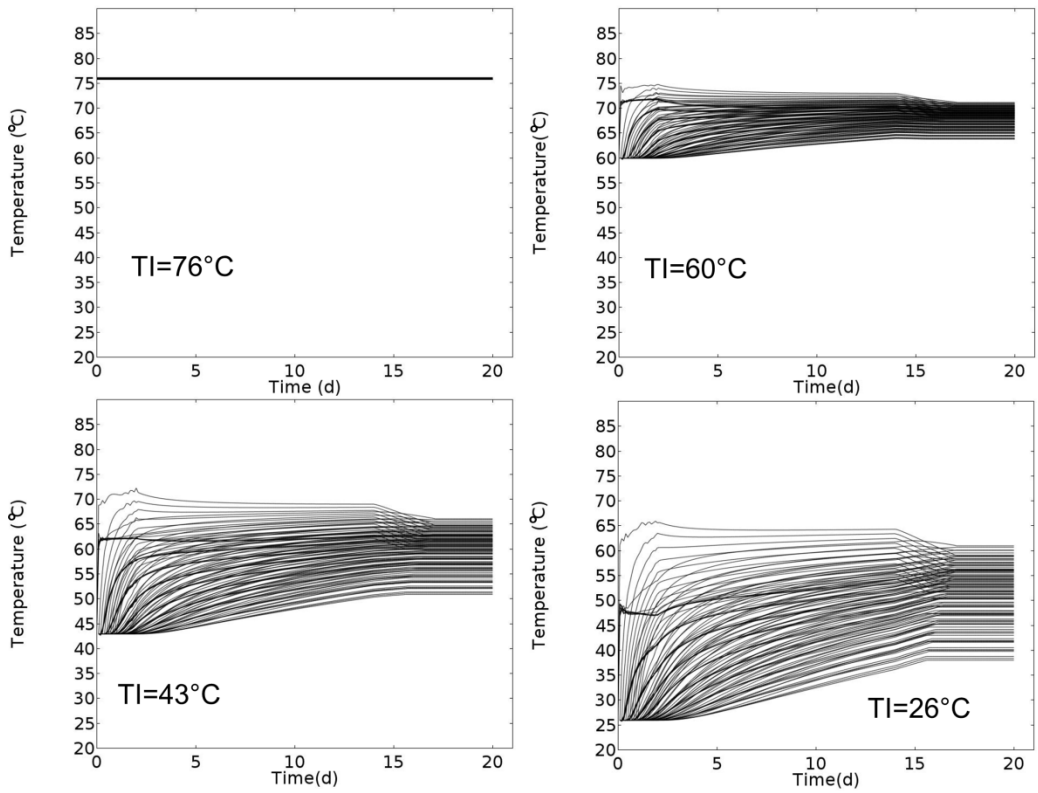

Figure 7. Individual nanoparticle temperature histories for injection temperatures equal to 76, 60, 43 and 26 °C as a function of time. 100 nanoparticles are injected evenly distributed in space (vertical) and time (horizontal) during the injection period of one day. The reservoir temperature is 76 °C. The figure depicts the nanoparticles' temperature as they move into the target formation, pause and return to the wellbore.

With the temperature histories illustrated in Fig. 7 and the degradation parameters in Table 1, we have calculated the relative fluorescence (=I since we have set I_0=1) of each nanoparticle (Fig. 8).

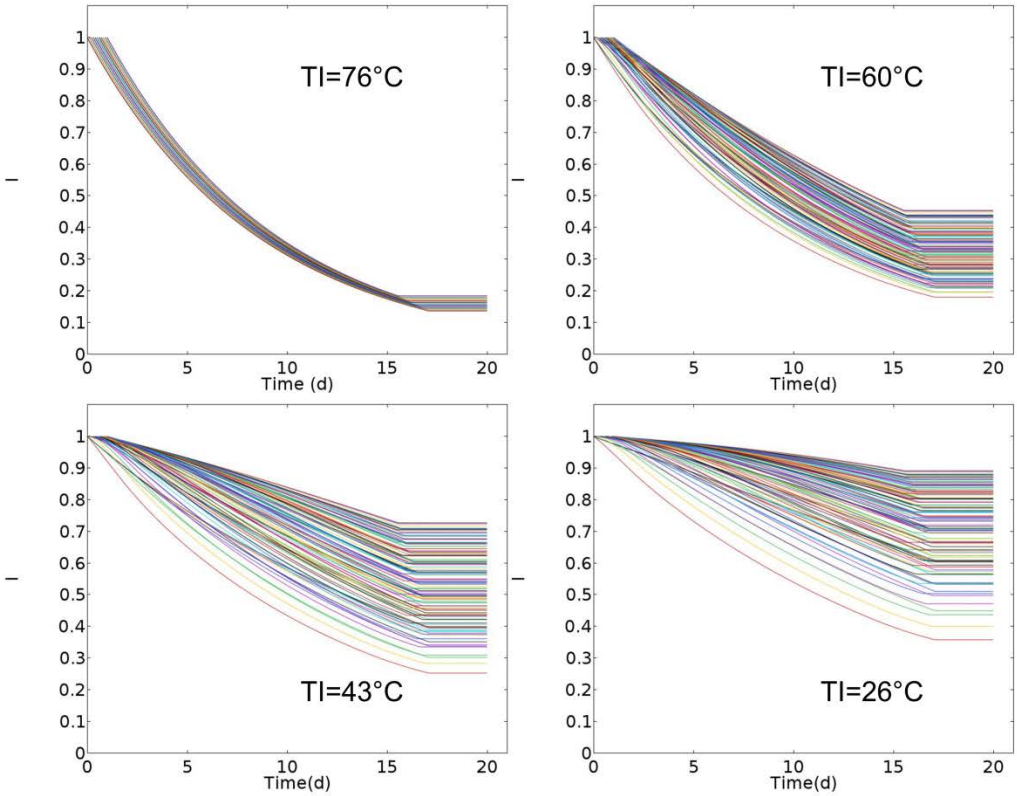

Figure 8. Fluorescence degradation as function of time for various injection temperatures. The lower the injection temperature, the less degradation there is in the dye's fluorescence. The differences are so large that they should be easily detectable in the back-produced fluid. The reservoir temperature is 76 °C. The figure depicts the nanoparticles' decrease in relative fluorescence (I) as they move into the target formation, pause and return to the wellbore.

Since the degradation rate depends exponentially on temperature, the degradation is much smaller for low injection temperatures than for high temperatures. The degradation calculation for an individual particle is terminated when it returns to the well. In reality, there will be some thermal decay also in the wellbore. However, since the particle's temperature will fall rapidly as it moves towards the Earth's surface, and the fluorescence degradation depends exponentially on temperature, this simplification should cause only an insignificant underestimation of the true degradation in the nanoparticles' fluorescence.

Finally, Fig. 9 shows the aggregate average relative fluorescence of all the nanoparticles together with their standard deviation.

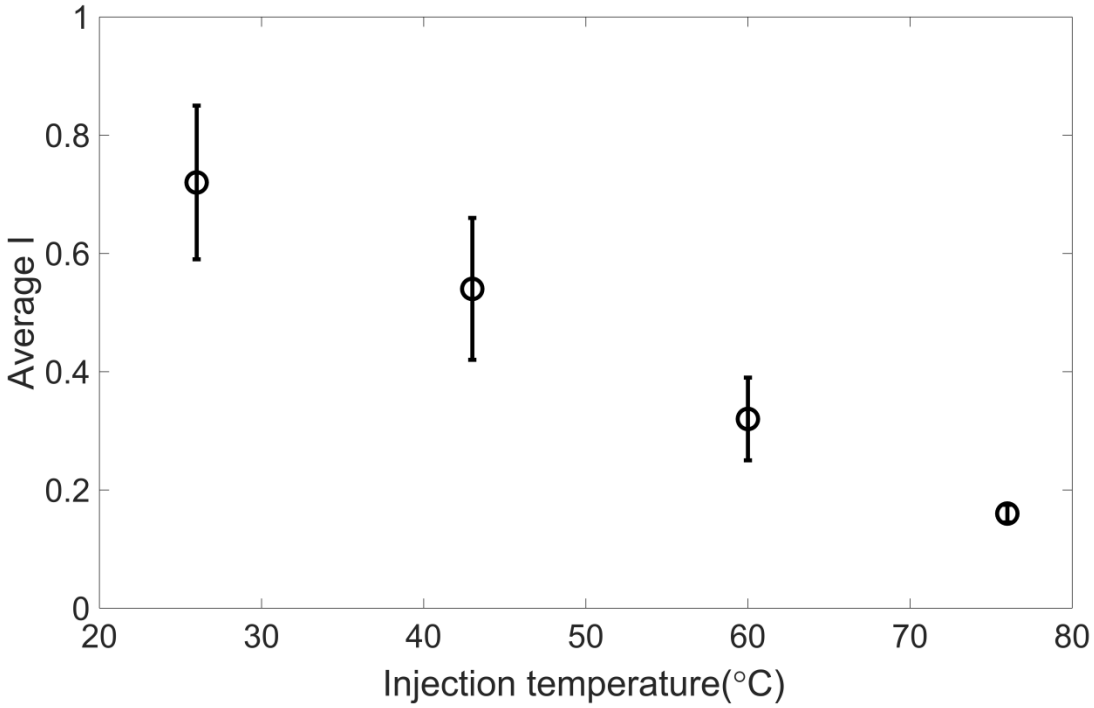

Figure 9. Average relative fluorescence and standard deviation of nanoparticle at the end of the SWCT test for injection temperatures of 26, 43, 60 and 76 °C. The higher the injection temperature, the larger the fluorescence degradation.

If the designed nanotracers had been injected together with the primary tracer in Deans and Majoros (1980)'s Field Test#3, and we had observed their fluorescence after the test, we would have had the necessary temperature constraint to arrive at the correct S_{or} estimate. In other words, properly designed nanoparticles could finally provide the independent 'temperature history data' called for by Park almost 30 years ago (Park, 1989).

5. Discussion

If nanoparticles that comply with the design criteria presented above could not be realized, our study would have only academic interest. However, there are positive indications that such particles indeed can be produced. Agenet et al. (2012) enclosed a lanthanide complex (Eu-DTPA) and the organic dye FITC (fluorescein isothiocyanate) in a silica nanoparticle with a size distribution centered around 60 nm. The lanthanide complex serves as a reference whereas FITC experiences thermal degradation during heating. In preliminary heating studies, Agenet et al. (2012) do indeed find that the fluorescence of Eu-DTPA does not seem to decay upon heating whereas the dye appears to degrade (their Fig. 8). Using a similar particle configuration, the heating studies of Brichart (2016) indicate a half-life of the temperature sensitive component equal to nineteen days at 70 °C and seven days at 90 °C. With the pre-exponential factor and activation energy used in Fig. 5, the half-lives are eight and three days, respectively. Consequently, had we used the results of Brichart (2016) in our thermal decay calculations, the

reduction in fluorescence during the SWCT test would have been somewhat smaller than observed in Figs. 8 and 9.

Agenet et al. (2012) also performed flooding studies with their nanoparticles in an oil-free Bentheimer sandstone core at room temperature. The results indicate that the particles move more or less with the injection fluid (i.e., it is a quasi-ideal water tracer). Rather few experiments were, however, performed. More importantly, since the purpose of a SWCT test is to quantify the amount of residual oil, it is the particles distribution to the oil that is most relevant, and not to the rock matrix. Fletcher and Holt (2011) discuss how silanization of silica nanoparticles yields controllable hydrophobization. This could be a fruitful approach towards synthesizing silica nanoparticles with desired distribution constants between water and oil. More generally, the transport properties of the silica nanoparticles at other temperatures, in other lithologies (including carbonates), etc. have been relatively little investigated. In future flooding studies, the importance of particle size and nanoparticle concentration for the transport and retention should be considered (e.g., Wang et al., 2012).

In our numerical calculations, we have used different but constant injection temperatures. The main reason for this decision was that we wished to utilize the S_{or} estimates of Park (1989) who used the same assumption. Future studies could use wellbore temperature models as discussed by for example Ramey (1962) and Chen and Novotny (2003). In such models, the injection temperature will change with time and will depend on the initial temperature condition, well- and rock thermal properties, injection rates etc. It seems to us that the temperature history nanoparticles would be even more useful in such a more complex scenario.

One might argue that good analytical or numerical models of the temperature of the fluid in the injection well could make the use of temperature nanotracers as discussed in this paper *less* useful. However, such calculations depend on a large number of often poorly constrained parameters (e.g., Ying et al., 2008). Moreover, as discussed above, the temperature history of injected fluid depends also on the target formation's effective thickness and other factors. Since most SWCT tests are performed in producers, the temperature distribution within and near the well will depend on the well's production history.

Since in the halogen-acid salts-CO_2 version of the SWCT method (Wellington and Richardson, 1994) the primary tracer moves with the oil, there will normally be no overlap between it and the temperature front (cf. Fig. 6). Thus, there will be no (significant) temperature gradient across the primary tracer bank that affects its hydrolysis. Notwithstanding, we think that also in such a scenario, temperature history nanoparticles may provide interesting information on for example the effective thickness of the target formation.

The methodology developed in this paper was aimed at investigating the applicability of the designed nanoparticles in SWCT tests. It has in no way been optimized for extracting maximum information from the data provided by the nanoparticles. For instance, we have only used the average (and standard deviation) relative fluorescence of all the nanoparticles lumped together. Clearly, more information could be derived from the nanoparticle data if their fluorescence as a function of time was monitored in the produced fluid at the well site. We think that combining statistical experimental design (e.g., Montgomery, 2013) in the planning phase of a SWCT test

with mathematical inversion methods (e.g., Menke, 1989) for analysis of the joint tracer (primary, secondary, others) and nanoparticle data sets is a good candidate for optimizing the methodology outlined in our work. We hypotize that this could be particularly advantageous for extracting model attributes like the effective thickness of the target formation. Also valuable information on the wellbore and its thermal interaction with the surrounding rocks might in principle be obtained by more advanced methods. More elaborate studies are needed to confirm or reject this proposition.

Hopefully, our work may contribute to encourage research institutions and companies to realize the as yet hypothetical nanoparticles. When these are available, we would like to translate our theoretical work into a practical field test.

6. Conclusions

The time and money needed to develop new nanoparticles are substantial and in our view it may be wise to reallocate more resources into studies of how the nanoparticles should de designed in order to be really useful for solving an identified problem. In particular, we believe that it is a good idea to demonstrate the usefulness of as yet hypothetical nanoparticles by performing computer simulations of the system at hand with them. To illustrate this idea, we discuss a well-defined and relatively simple system, namely the SWCT test, the purpose of which is to estimate the residual oil saturation in the vicinity of a well.

A temperature gradient may develop across the primary tracer bank in SWCT tests. Because the hydrolysis rate of the primary tracer typically increases exponentially with temperature, this may cause a displacement of the produced secondary tracer relative to the primary tracer that must be taken into account if S_{or} is to be estimated correctly. Hitherto, there has been a lack of tools to assess the temperature history of the tracer bank. Progress in nanotechnology may finally provide a solution to this problem.

We have developed design criteria for nanoparticles that may serve as temperature constraints in SWCT tests. An axis-symmetrical numerical model is used to demonstrate the usefulness of the as yet hypothetical nanoparticles based on data from a published SWCT test. We demonstrate that the novel nanoparticles may improve S_{or} estimates. In addition, they may potentially also yield valuable information on the effective thickness and other characteristics of the target formation, the surrounding rock and perhaps even on the wellbore and its thermal interaction with the surroundings.

7. Appendix A

Dispersion of the nanoparticles is neglected since this would only have an insignificant impact on the results. According to the Stokes-Einstein-Sutherland equation, the diffusion constant, D_m, of a nanoparticle can be calculated from the formula

$$D_m = k_B T / 3\pi\eta d \tag{A1}$$

in which k_B is the Boltzmann constant, T is again temperature (in K), η is viscosity and d is the diameter of the nanoparticle. In water at 75 °C, this yields D_m=5.1 10^{-12} m^2s^{-1} for d=100 nm. We may estimate the longitudinal dispersion coefficient, D_L, from the equation (Coutelieris and Delgado, 2012)

$$D_L = D_m/\tau \ + 0.5vd_r \tag{A2}$$

where τ is the tortuosity, v is the nanoparticle velocity and d_r is the diameter of the sandstone grains. For a tortuosity of two and a grain diameter equal to 3.0 10^{-4} m appropriate for a medium fine sand (e.g., Nelson, 2009), and the velocity from Eq. 4, we have that D_L is of the order of 10^{-9}-10^{-10} m^2s^{-1}. However, for the corresponding Peclet numbers, experimental studies indicate that Eq. A2 will underestimate D_L (Coutelieris and Delgado, 2012). Judging from their Fig. 46.6, a better estimate is that D_L is of the order of 10^{-8} m^2s^{-1}. This implies that the dispersion length will be about $\sqrt{D_L 6\ days}$~0.1 m during the total duration of the injection and production phases. Since this is much smaller than the spatial length of the primary tracer bank (Fig. 6), we conclude that dispersion will be insignificant. During the shut-in period, it's D_m that matters and the diffusion will be neglible.

8. Acknowledgements

Two anonymous reviewers provided constructive remarks on the manuscript. Thanks are also due Jan Nossen, Sissel O. Viig, Tor Bjørnstad and Netaji R. Kesana for useful comments. This work was financed by Institute for energy technology's Strategic Institute Program.

9. References

Adams, M.C. and Davis, J., 1991. Kinetics of fluorescein decay and its application as a geothermal tracer. Geothermics, 20, 53-66.

Agenet, N., Perriat, P., Brichart, T., Crowther, N., Martini, M. and Tillement, O., 2012. Fluorescent nanobeads: a first step toward intelligent water tracers. SPE International Oilfield Nanotechnology Conference, 12-14 June, Noordwijk, The Netherlands (2012).

Brichart, T., 2016. Can fluorescent nano-objects be used as reservoir tracers?, 26.4, IOR Norway, Stavanger, Norway (2016).

Chen, Z. and Novotny, R.J., 2003. Accurate prediction wellbore transient temperature profile under multiple temperature gradients: finite difference approach and case history. SPE Annual Technical Conference and Exhibition, 5-8 October, Denver, Colorado, USA (2003).

COMSOL Multiphysics, 2016. User Guide.

Coutelieres, F.A. and Delgado, J.M.P.Q., 2012. Advanced structured materials. Transport processes in porous media. Springer, Heidelberg.

Deans, H.A., 1971. Method of Determining Fluid Saturations in Reservoirs. U.S. Patent 3,623,842.

Deans, H.A. and Majoros, S., 1980. The single-well chemical tracer method for measuring residual oil saturation. Final report. U.S. Department of energy.

Elimelech, M., Gregory, J., Jia, X. and Williams, R.A., 1995. Particle deposition and aggregation. Measurement, modelling and simulation, Butterworth Heinemann, Woburn.

Fadeel, B., 2013. Nanosafety: towards safer design of nanomedicines. J. Internal Medicine, 274, 6, 578-580.

Fletcher, A.J.P. and Davis, J.P., 2010. How EOR can be Transformed by Nanotechnology. The 2010 SPE Improved Oil Recovery Symposium, 24-28 April, Tulsa, Oklahoma, USA (2010).

Fletcher, P.D.I. and Holt, B.I., 2011. Controlled silanization of silica nanoparticles to stabilize foams, climbing films, and liquid marbles. Langmuir, 27, 12869–12876.

Friedheim, J., Young, S., De Stefano, G., Lee, J. and Guo, Q., 2012. Nanotechnology for oilfield applications – hype or reality? SPE International Oilfield Nanotechnology Conference, 12-14 June, Noordwijk, The Netherlands (2012).

Gadgil, A.G., 1979. The single-well chemical tracer test in petroleum reservoirs with multicomponent, two-phase flow effects. PhD thesis, Rice University.

Interstate Oil Compact Commission, 1978. Determination of Residual Oil Saturation, Oklahoma City.

Kanji, M.Y., Funk, J.J. and Al-Yousif, Z., 2009. Nanofluid Coreflood Experiments in the ARAB-D. 2009 SPE Saudi Arabia Section Technical Symposium and Exhibition, 9-11 May, AlKobar, Saudi Arabia (2009).

Kong, A., and Ohadi, M.M., 2010. Applications of Micro and Nano Technologies in the Oil and Gas Industry – An Overview of the Recent Progress. Abu Dhabi International Petroleum Exhibition and Conference, 1-4 November, Abu Dhabi, UAE (2010).

McAdams, W.H., 1954. Heat transmission. McGraw-Hill Book Company, New York.

Menke, W., 1989. Geophysical data analysis: discrete inverse theory. Academic Press, San Diego.

Montgomery, D.C., 2012. Design and analysis of experiments. John Wiley and Sons, Inc., New York.

Nelson, P.H., 2009. Pore-throat sizes in sandstones, tight sandstones, and shales. Am. Ass. Petrol. Geol. Bull., 93, 3, 329-340.

Park, Y.J., 1989. Thermal effects of single-well chemical tracer tests for measuring residual oil saturation. PhD Thesis, University of Houston.

Park, Y.J., Deans, H.A. and Tezduyar, T.E., 1990. Finite element formulation for transport equations in a mixed co-ordinate system: an application to determine temperature effects on the single-well chemical tracer test. Int. J. Num. Methods in fluids, 11, 769-790.

Park, Y.J., Deans, H.A. and Tezduyar, T.E., 1991. Thermal effects on single-well chemical tracer tests for measuring residual oil saturation. SPE Formation Evaluation, 6, 401-408.

Ramey, Jr., H.J., 1962. Wellbore heat transmission. J. Petrol. Technol., 96, 427-435.

Rassenfoss, S., 2012. Illuminating the reservoir. J. Petrol. Technol., June 2012, 48-56.

Salathiel, R.A., 1973. Oil recovery by surface film drainage in mixed-wettability rocks. Trans. AIME, 225, 1216-1224.

Sheely, C.Q. and Baldwin, D.E., 1988. Single-well tracer tests for evaluating chemical enhanced oil recovery processes. J. Petrol. Technol., 1887-1896.

Smart, P.L. and Laidlaw, I.M.S., 1977. An evaluation of some fluorescent dyes for water tracing. Water Resources Res., 13, 1, 15-33.

Tezduyar, T.E., Park, Y.J. and Deans, H.A., 1987. Finite element procedures for time-dependent convection-diffusion-reaction systems. Int. J. Num. Methods in fluids, 7, 1013-1033.

Tomich, J.F., Dalton, Jr., R.L., Deans, H.A. and Shallenberger, L.K., 1973. Single-well tracer method to measure residual oil saturation. J. Petrol. Geol., 211-218.

Wang, C., Bobba, A.D., Attinti, R., Shen,C., Lazouskaya, V., Wang, L.-P., and Jin, Y., 2012. Retention and transport of silica nanoparticles in saturated porous media: effect of concentration and particle size. Environ. Sci. Technol., 46, 7151−7158.

Wellington, S.L. and Richardson, E.A., 1994. Redesigned ester single-well tracer test that incorporates pH-driven hydrolysis rate changes. SPE Reservoir Engineering, 233-239.

Wyckoff, R.D. and Botset, H.G., 1936. The flow of gas-liquid mixtures through unconsolidated sands. Phys., 7, 325-345.

Ying. S., Yanjie, S. and Hong, L., 2008. Numerical simulation of downhole temperature distribution in producing oil wells. Appl. geophys., 5,4, 340 – 349.

Yu, J., Berlin, J.M., Lu, W., Zhang, L., Kan, A.T., Zhang, P., Walsh, E.E., Work, S.N., Chen, W., Tour, J.M. Wong, M.S., Tomson, M.B., 2010. Transport Study of Nanoparticles for Oilfield Applications. SPE International Conference on Oilfield Scale, 26-27 May, Aberdeen, United Kingdom (2010).